Supplement of The Cryosphere, 12, 851–866, 2018
https://doi.org/10.5194/tc-12-851-2018-supplement

The Cryosphere Open Access EGU

Supplement of

An investigation of the thermomechanical features of Laohugou Glacier No. 12 on Qilian Shan, western China, using a two-dimensional first-order flow-band ice flow model

Yuzhe Wang et al.

Correspondence to: Tong Zhang (zhangtong@cma.gov.cn)

Reconstruction of air temperature for LHG12

We collected historical air temperature data from five meteorological stations (MS) surrounding LHG12 (Tab. 1). We also processed the observed air temperature data at two AWSs deployed on LHG12 (see Fig. 1 in the manuscript).The two AWSs were named as AWS4550 and AWS5040 based on their altitudes. The correlation coefficients between the daily air temperature of MSs and that of AWS4550 during 2010–2013 were then calculated (Tab. 1). We can see that there is the best correlation between the data of Tuole Station and AWS4550 (Tab. 1, Fig. 1). Therefore, we used the daily air temperature during 1956–2013 at Tuole Station to reconstruct the air temperature of LHG12.

We calculated the monthly mean air temperature lapse rates between Tuole Station and AWSs on the glacier over the period of 2009–2013 (Fig. 2). The monthly mean lapse rates calculated between Tuole and AWS4550 (γ_1^T) are not consistent with those calculated between Tuole and AWS5040 (γ_2^T). We used the mean value (γ^T) of γ_1^T and γ_2^T to extrapolate the daily air temperature at Tuole Station to LHG12 as follows:

$$T_{\mathrm{LHG12},z,i} = T_{\mathrm{TL},i} + \gamma_j^T \cdot (z - z_{\mathrm{TL}}), \tag{1}$$

where $T_{\mathrm{LHG12},z,i}$ is the air temperature of day i at the elevation z, $T_{\mathrm{TL},i}$ is the air temperature of Tuole Station of day i, γ_j^T is the air temperature lapse rate of month j, and z_{TL} is the elevation of Tuole Station. Fig. 3a shows the reconstructed annual mean air temperature at 4550 m a.s.l. during 1957–2013. The differences of annual mean air temperatures between the AWS measured and the reconstructed are less than 0.53°C (Fig. 3a), and the standard deviation of the differences of daily air temperatures at 4550 m a.s.l. between the measured and the reconstructed is about 0.41°C (Fig. 3b), indicating a robust reconstruction of the daily air temperature on LHG12.

Table 1: Correlation coefficients between the daily air temperatures of AWS at 4550 m a.s.l. and those of selected meteorological stations. Information of the selected meteorological stations are also indicated.

Station	Latitude (N)	Longitude (E)	Elevation (m a.s.l.)	2010	2011	2012	2013
Dunhuang	40°09’	94°41’	1139	0.94	0.94	0.94	0.92
Guazhou	40°32’	95°46’	1171	0.94	0.95	0.95	0.93
Jiuquan	39°46’	98°29’	1477	0.93	0.94	0.94	0.92
Tuole	38°48’	98°25’	3367	0.97	0.97	0.97	0.94
Yumenzhen	40°16’	97°02’	1526	0.94	0.95	0.95	0.92

The reanalysis data of precipitation on LHG12

We used the CAPD (China alpine region month precipitation data set) precipitation dataset in Qilian Shan to get the precipitation on LHG12. The CAPD

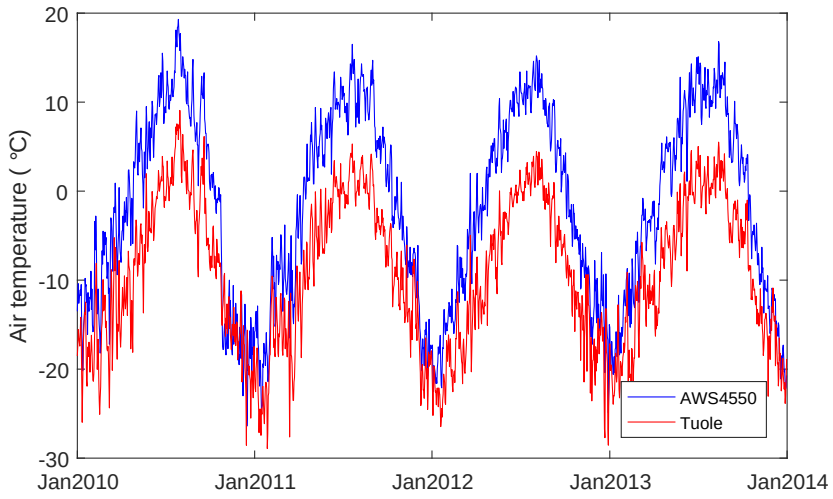

Figure 1: Comparison of daily air temperatures at the AWS4550 (blue line) with those at Tuole Station (red line) during the period 2010–2013.

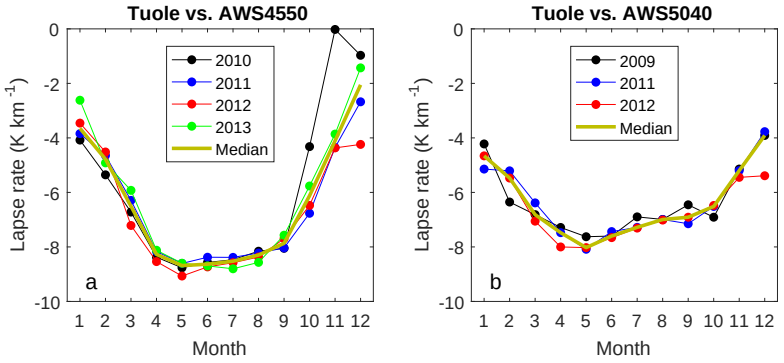

Figure 2: (a) Monthly mean air temperature lapse rates between Tuole Station and AWS4550, i.e. γ_1^T in 2010, 2011, 2012 and 2013. (b) Monthly mean air temperature lapse rates between Tuole Station and AWS5040, i.e. γ_1^T in 2009, 2011 and 2012.

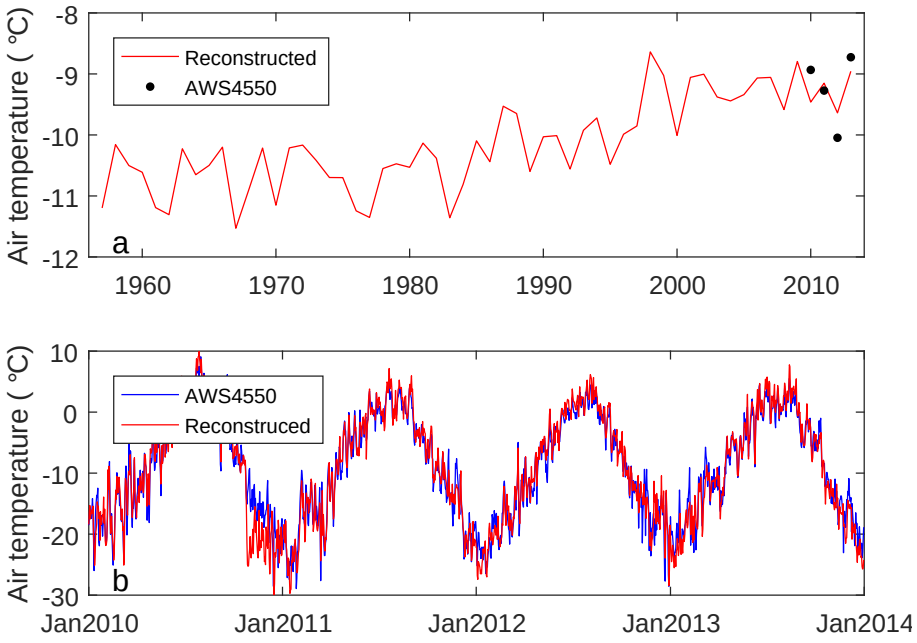

Figure 3: (a) Reconstructed annual mean air temperatures at 4550 m a.s.l. The black dots indicate the annual mean air temperatures measured by the AWS at 4550 m a.s.l. (b) Comparison of the daily air temperatures between the reconstructed (red line) and measured (blue line).

was generated using all available precipitation data in the Qilian Shan (Chen et al., 2015), and provided the monthly sum of precipitation during the period of 1960–2013 on a 1 km × 1 km grid (Fig. 4). We chose 91 grid points surrounding LHG12, and calculated the monthly mean precipitation gradients γ^P in 1960–2013. The monthly sum of precipitation on LHG12 at the elevation z in month j, $P_{z,j}$, is calculated as

$$P_{z,j} = P_{\mathrm{ref},j} + \gamma_j^P (z - z_{\mathrm{ref}}), \tag{2}$$

where $P_{\mathrm{ref},j}$ is the monthly sum precipitation at a reference site of month j, z_{ref} is the elevation of the reference site, and γ_j^P is the monthly mean precipitation gradient of month j.

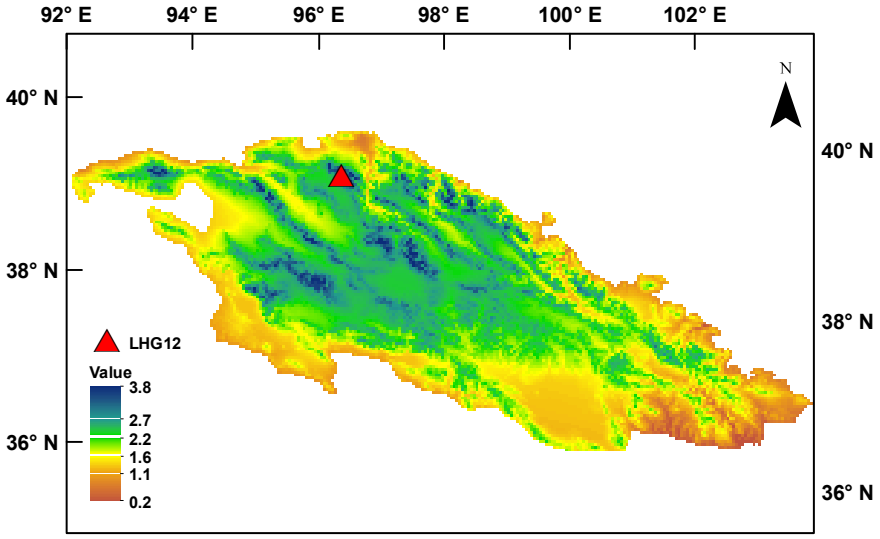

Figure 4: An example of the gridded precipitation dataset (CPAD) in Qilian Shan.

Parameter sensitivities of the surface mass balance model

Figures. 5–8 show the parameter sensitivities of the surface mass balance model. The model results are compared with the observed mass balance in 2010–2011 and 2011–2012. We finally adopt a set of parameters, i.e. $k_i = 6$ mm K d^{-1}, $k_s = 4$ mm K d^{-1}, $T_m = -1.45$ °C, $f_P = 0.6$, $T_{\mathrm{crit1}} = -1.05$ °C, and $T_{\mathrm{crit2}} =$

0.64 °C. It should be noted that the adopted ice and snow degree-day factors are within the range of measured values in western China (Zhang et al., 2006; Wang et al., 2017).

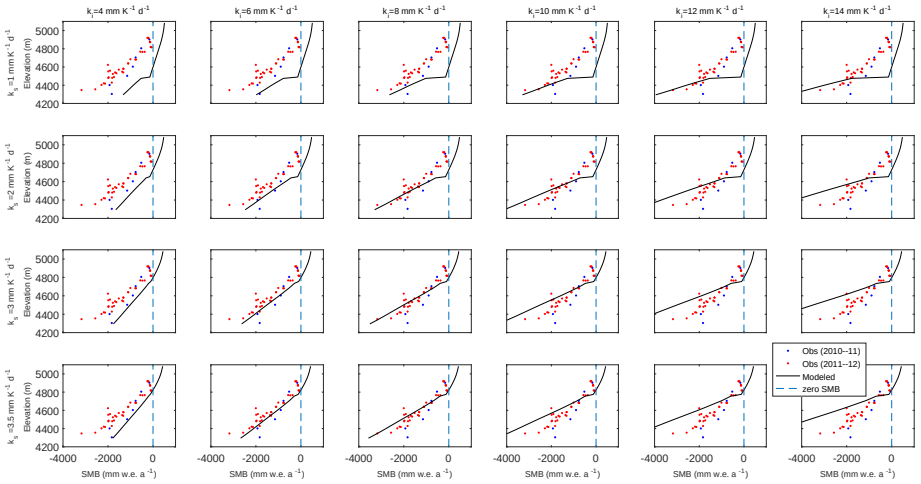

Figure 5: Sensitivities of ice (k_i) and snow (k_s) degree-day factors in the surface mass balance model. Model results are compared with observed surface mass balances at the balance years of 2010–2011 and 2011–2012.

Surface relaxation

Figure 9 shows the evolutions of surface horizontal velocity (u_s), surface vertical velocity (w_s), and ice thickness (H) during the relaxation. Both u_s and w_s become smooth after the relaxation (Fig. 9a, b). Significant thinning of the ice thickness occurs in the regions of km 0–2.1 and km 2.7–3.5, while ice thickening mainly occurs in the region of km 3.5–6.5 (Fig. 9c).

Glacier surface elevation change during 1957–2014

Figure 10 shows the surface elevation changes of LHG12 along the center flowline during 1957–2014. The noticeable changes of ice thickness are mainly in km 7 – 9 (below the confluence area, 4600 m a.s.l.).

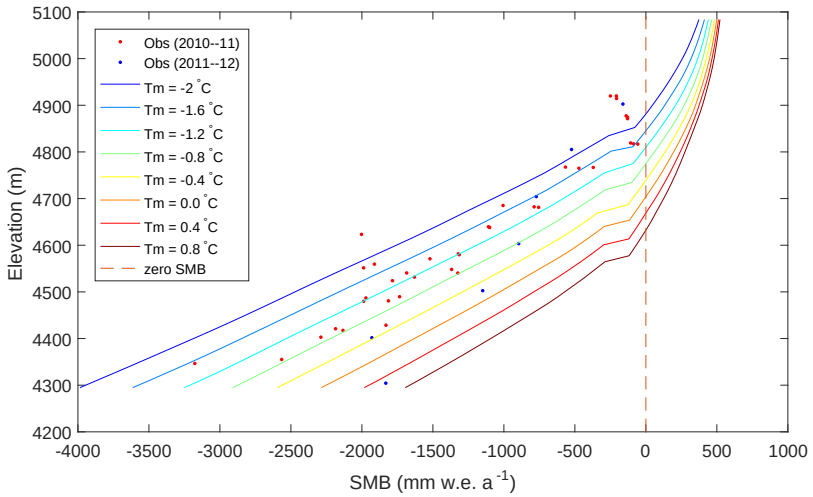

Figure 6: Sensitivity of the parameter T_m in the surface mass balance model.

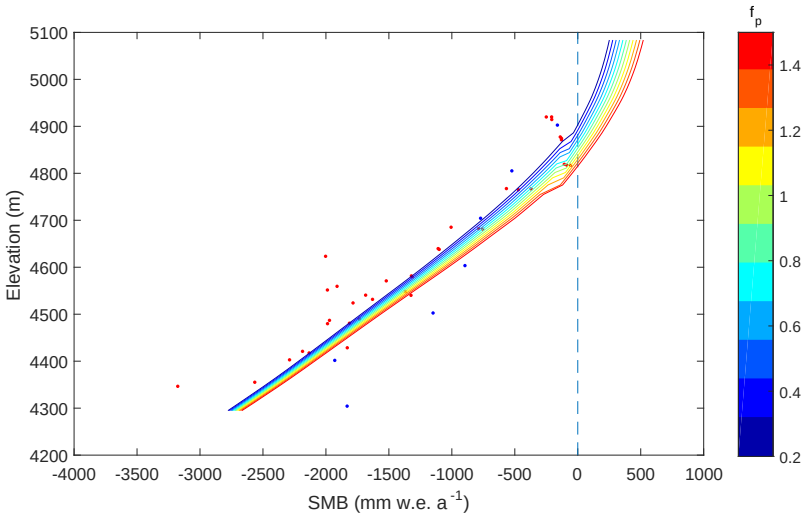

Figure 7: Sensitivity of the parameter f_P in the surface mass balance model.

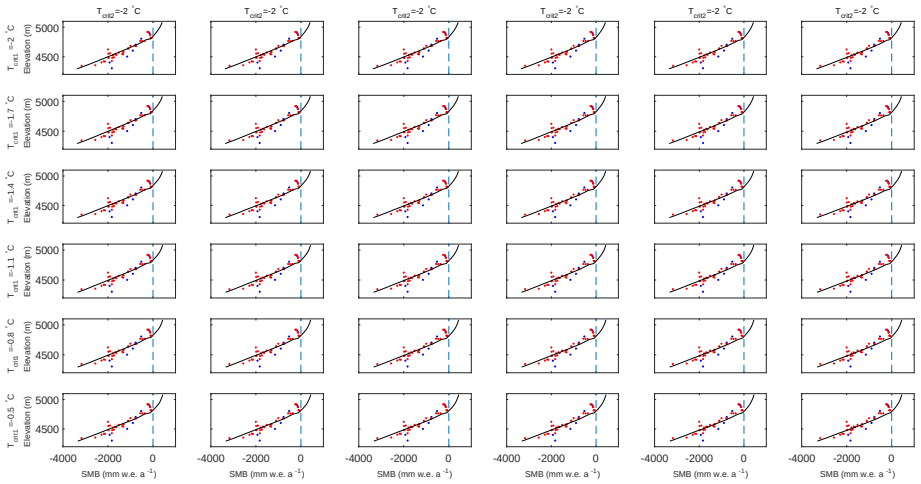

Figure 8: Sensitivities of the threshold temperatures, T_{crit1} and T_{crit2} in the surface mass balance model.

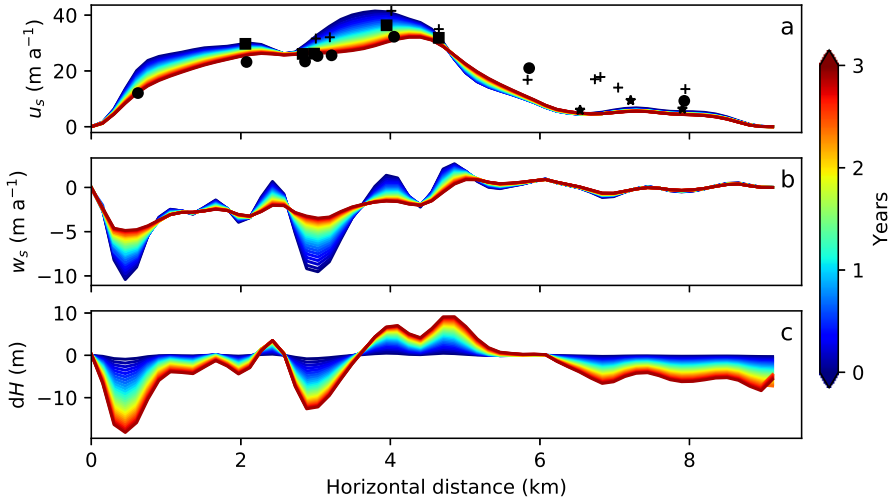

Figure 9: Changes of surface horizontal velocity (a), surface vertical velocity (b), and ice thickness (c) during the 3-year relaxation of the free surface.

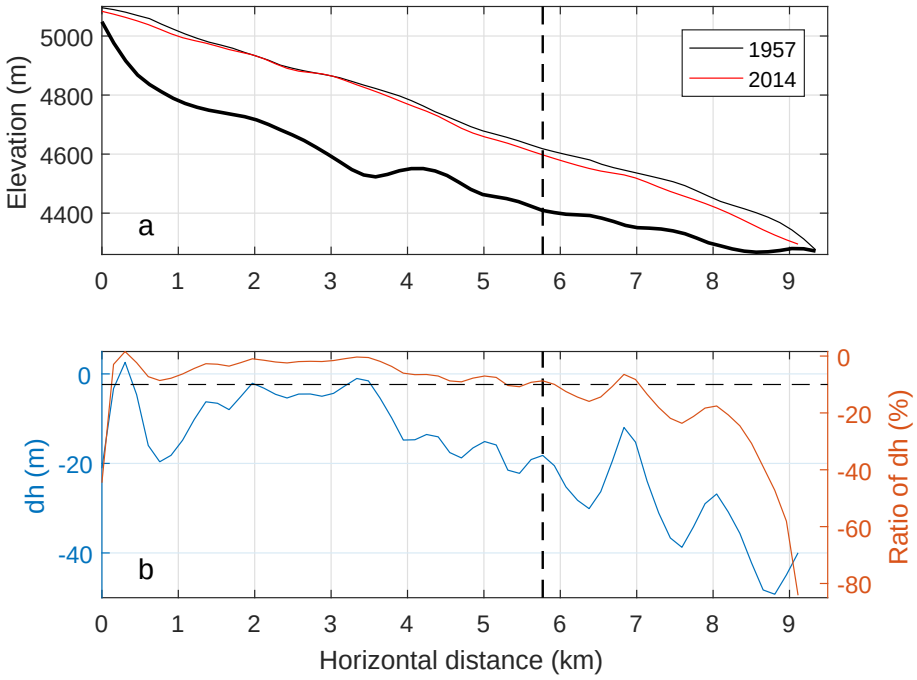

Figure 10: (a) The geometries of LHG12 along the center flowline in 1957 (black line) and 2014 (red line). The surface elevation in 1957 was extracted from a 1:50,000 contour map, while the surface elevation in 2014 was measured using South Lingrui S82 GPS system. Dashed line indicates the boundary between the east tributary and the confluence area. (b) Left y axis indicates the elevation differences (dh) during 1957–2014, while right y axis indicates the ratio of dh to ice thickness.

References

Chen, R., Liu, J., Kang, E., Yang, Y., Han, C., Liu, Z., Song, Y., Qing, W., and Zhu, P.: Precipitation measurement intercomparison in the Qilian Mountains, north-eastern Tibetan Plateau, The Cryosphere, 9, 1995–2008, doi:10.5194/tc-9-1995-2015, 2015.

Wang, S., Yao, T., Tian, L., and Pu, J.: Glacier mass variation and its effect on surface runoff in the Beida River catchment during 1957-2013, Journal of Glaciology, 69, 1–12, doi:10.1017/jog.2017.13, 2017.

Zhang, Y., Liu, S., and Ding, Y.: Observed degree-day factors and their spatial variation on glaciers in western China, Annals of Glaciology, 43, 301–306, doi:10.3189/172756406781811952, 2006.